

# Hydrogen-Oxygen Flame Acceleration in Channels of Different Widths and Deflagration-to-Detonation Transitions for a Detailed Chemical Reaction Models

M. F. Ivanov<sup>1</sup>, A. D. Kiverin<sup>1</sup>, M. A. Liberman<sup>2,3</sup>

<sup>1</sup> Joint Institute for High Temperatures, Russian Academy of Science, Moscow, Russia

<sup>2</sup> Skobeltsyn Institute of Nuclear Physics, Moscow State University, Moscow, 119991 Russia

<sup>3</sup> Department of Physics, Uppsala University, Box 530, 751 21, Uppsala, Sweden

## 1 Introduction

The present work focuses on the features of the flame acceleration and the upstream flow forming ahead of the flame propagating in channels of different widths. The objectives are to examine effect of the channel width on the flame propagation dynamics, the flame acceleration in channels of different widths, shock wave formation in the upstream flow, and origin of the transitions from deflagration to detonation in hydrogen/oxygen mixture with a detailed chemical kinetic model. Over the years there has been significant progress made in the understanding of the flame acceleration thanks to theoretical, experimental and numerical studies [1-8]. However, conclusions drawn from the previous studies were mainly based on a simplified one-step chemical model. However, a single-step reaction model cannot reproduce the main properties of the combustion and the flow such as the induction time in chain-branching kinetics and detonation initiation. It is therefore important to investigate the qualitative and quantitative differences of the processes between chain-branching kinetics and the predictions from one-step models. In the present work we show that the flame acceleration in channels with no-slip walls is entirely determined by the features of the flow formed ahead of the flame which are different for a wide channel and for the channel of width smaller than some critical value. Results of the high resolution simulations and theoretical analysis are consistent with experimental investigations of the combustion in ethylene-oxygen [9] and hydrogen-oxygen [10] highly reactive gaseous mixtures.

## 2 Formulation of the problem, numerical method and results

The simulations modeled a flame ignited at the closed end and then propagating to the open end of the two-dimensional rectangular channel of widths from 10mm to 0.5mm with smooth no-slip walls. Initial temperature and pressure were  $T_0 = 298\text{K}$ ,  $P_0 = 1.0\text{bar}$ . The computations solved the two-dimensional, time-dependent, reactive Navier-Stokes equations for compressible flow including the effects of viscosity, thermal conduction, molecular diffusion, real equation of state and detailed chemical kinetics for the reactive species  $\text{H}_2$ ,  $\text{O}_2$ ,  $\text{H}$ ,  $\text{O}$ ,  $\text{OH}$ ,  $\text{H}_2\text{O}$ ,  $\text{H}_2\text{O}_2$ , and  $\text{HO}_2$  with subsequent chain branching and energy release [4, 5]. The equations of state for the reactive species and combustion products were taken with the temperature dependence of the specific heats, heat capacities and enthalpies of each species borrowed from the JANAF tables. The viscosity and thermal

conductivity coefficients of the mixture are calculated using the Lennard-Jones potential. Coefficients of the heat conduction of  $i$ -th species  $\kappa_i = \mu_i c_{pi} / Pr$  are expressed via the viscosity  $\mu_i$  and the Prandtl number:  $Pr = 0.75$ . The reaction scheme for a stoichiometric  $H_2-O_2$  mixture used in the simulations has been proved to be adequate to complete chemical kinetic scheme. The computed thermodynamic, chemical, and material parameters using this chemical scheme are in a good agreement with the flame and detonation wave characteristics measured experimentally. The computational method was described and tested extensively in [11, 12]. Its validation, convergence and resolution taken to resolve the structure of the flame front with the meshes up to 64 computational cells per flame width are presented in [13].

Figure 1 shows the flame velocity-time dependence and the transition to detonation calculated for channels of different widths. The plots in figure 1 demonstrate similar feature of three distinctive stages of the flame acceleration if the channel width  $D > 1\text{mm}$ : 1) a short stage of the exponential increase of the flame velocity (zoomed part is shown in the inset of figure 1 (left) for  $D=10\text{mm}$ ); 2) the second stage when the acceleration rate decreases compared with the first stage; 3) the sharp increase of the flame velocity and actual transition to detonation. On the contrary, scenario of the flame acceleration and DDT are different for channels of width  $D < 1\text{mm}$  (figure 2).

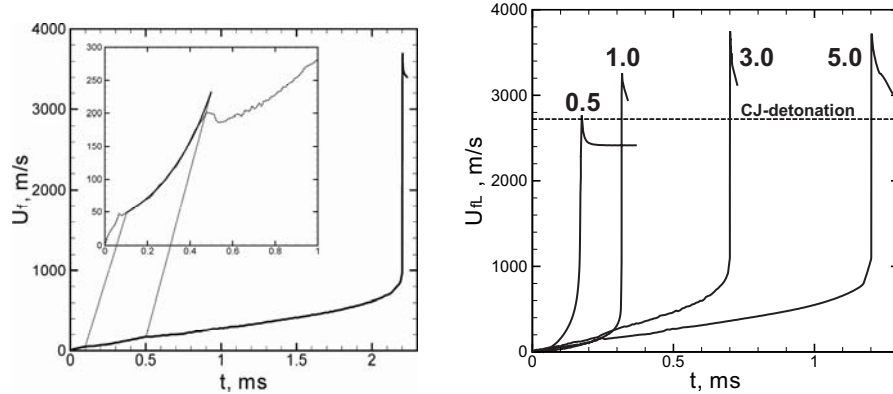


Figure 1. Computed flame speeds of  $H_2-O_2$  flames. Left:  $D=10\text{mm}$ , inset – zoomed image of exponential stage. Right: Computed flame speeds for channels  $D=0.5, 1, 3, 5\text{mm}$ .

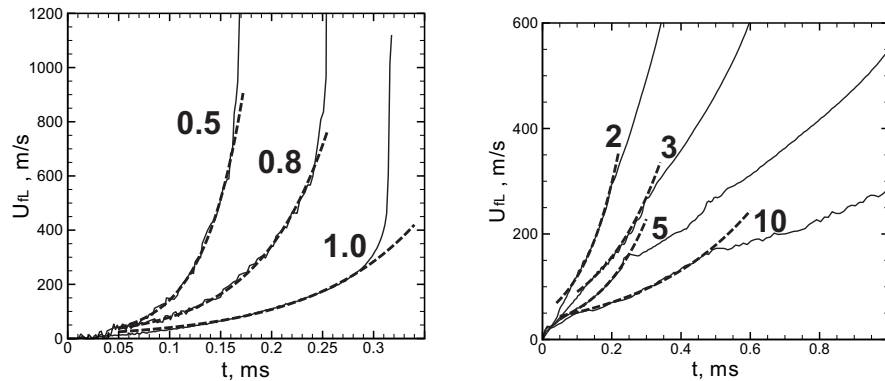


Figure 2. Enlargement of the flame velocity-time dependence channels  $D=0.5, 0.8, 1, 2, 3, 5$  and  $10\text{mm}$ . Dashed lines are exponential approximations  $U_{fl} = U_f \cdot \exp\{\alpha U_f t / D\}$ .

The difference in dynamics of the flame in a narrow and in a wide channels is clearly seen in figure 2 which shows zoomed images of the flame velocity-time dependences during the initial stages of the flame acceleration in the channels of widths  $D=0.5, 0.8, 1.0\text{mm}$  (left) and  $D=2, 3, 5, 10\text{mm}$  (right). For wider channels ( $D>1\text{mm}$ ), the initial stage can be approximated by the exponential increase of the flame velocity shown by the dashed lines turns into the stage of a slower acceleration, which can be described by a polynomial function  $U_{Lr} \propto a + bt^{n_1} + ct^{n_2} + \dots$  with  $n_i < 1$ . On the contrary, in thinner channels ( $D<1\text{mm}$ ) the exponential growth of the flame velocity (dashed lines figure 2, left) is not bounded in time and an initially subsonic deflagration wave may accelerate exponentially till the actual transition to detonation.

A propagating flame initiated near the closed end of the channel controls the flow forming ahead of it, which results in the flame acceleration compatible with the physical boundary conditions. The expansion of the high temperature burned gas induces an outward flow in the unburned reactants with the velocity  $u = (\Theta - 1)U_f$  while the flame propagates with the velocity  $U_{fL} = \Theta U_f$  in the laboratory reference of frame, where  $U_f$  is the normal velocity of laminar flame,  $\Theta = \rho_u / \rho_b \sim 10$  is the density ratio of the unburned  $\rho_u$  and burned  $\rho_b$  gases. For a wide channel the flow ahead of the flame is nearly uniform in the bulk, with the flow velocity dropping to zero at the channel walls within a thin boundary layer of the thickness  $\delta_1 \ll D$ . Every part of the flame front moves with respect to the fresh mixture with normal velocity  $U_f$  and simultaneously it is drifted with the local velocity of the flow ahead of the flame. As the flame front advances into a nonuniform velocity field, the flame surface is stretched taking the shape of the velocity profile in the flow ahead, and the flame surface increases. The stretched flame consumes fresh fuel over a larger surface area which results in an increase in the rate of heat release per unit projected flame area. A higher burning velocity results in an enhancement of the flow velocity ahead of the flame, which in turn gives rise to a larger gradient field and enhanced flame stretching, and so on. A positive feedback coupling is established between the upstream flow and the burning velocity as the flame is stretched in the velocity field ahead. The flame sheet “repeats” the shape of the upstream velocity profile remaining almost flat in the bulk with the edges of the flame skirt stretched backward within the boundary layer. Within the model of a thin flame the increase of the burning rate is proportional to the relative increase of the flame surface which grows linearly in time with accuracy  $\delta_1 / D \ll 1$  (2D case). The expression for the combustion wave velocity  $U_{fL} = \Theta U_f \cdot \exp\{\alpha U_f t / D\}$  is then similar to the expression for a “finger” flame velocity [14] with the numerical factor  $\alpha$  of the order of unity.

The distance between the flame and the shock generated by the flame ahead is  $(X_{sh} - X_f) \sim (5 - 10)D$ . For the Reynolds number  $Re = (\Theta - 1)U_f D / \nu \sim \Theta U_f D / \nu$  in the upstream flow thickness of the boundary layer can be estimated as  $\delta_1 \sim (X_{sh} - X_f) / \sqrt{Re}$ , where  $\nu$  is the kinematic viscosity coefficient. Therefore the condition  $\delta_1 / D \ll 1$  holds for  $Re \gg 1$ . The Poiseuille flow can be formed ahead of the flame for a very thin channels or slow flames. This requires thickness of the boundary layer  $\delta_1 \propto (X_{sh} - X_f) / \sqrt{Re} \sim 5D / \sqrt{Re}$  to be of the order of the channel width, which leads to  $Re \sim 25$ . It is convenient to express the Reynolds number in terms of the flame thickness  $L_f$  and the normal velocity of a laminar flame,  $Re \sim \Theta D / L_f$ . Taking for  $H_2\text{-}O_2$  at initial pressure  $P_0 = 1.0\text{bar}$ :  $L_f = 0.24\text{mm}$ ,  $U_f = 10\text{m/s}$ ,  $\Theta \sim 10$ ,  $L_f U_f \approx \nu$ , we obtain that the Poiseuille flow is established for  $D < 25L_f / \Theta \approx 1\text{mm}$ .

The difference of the flame dynamics in a wide and in a thin channel was observed experimentally in the measured velocity-time dependence. For wide channels there are three distinctive stages of the flame acceleration, while for thin channels there is only one stage of exponential acceleration, which ends up with the transition to detonation [9]. For experiments [9] with ethylene/oxygen at atmospheric

pressure,  $L_f = 0.075\text{mm}$ ,  $U_f = 5.5\text{m/s}$ ,  $\Theta = 14$  and the critical diameter when the flame dynamics is changed is about 0.35-0.4mm.

As the flame front is stretched along the walls in a wide channel, a narrow fold is formed within the boundary layer between the edges of the flame skirt and the wall. As the fold becomes deeper, the angle at the fold's tip became smaller, and parts of the flame near the fold's tip approach the wall. Because of either heat losses to the wall or increased velocity of the fold's tip the edges of the flame skirt near the walls will be shortened reducing the surface of the flame front area and thus decreasing the rate of the flame acceleration after  $t_2 \sim (L_f / U_f) \sqrt{D / \Theta L_f}$  [11]. Since  $t_2$  is short, the flame acceleration during the first stage is constant with accuracy of the first order terms  $L_f / D \ll 1$ . Therefore at  $t \geq t_2$  the velocity-time dependence can be approximated as  $U_{fl} = \Theta U_f [1 + \beta(t / \tau_f)^n]$ , with  $0 < n < 1$ . While during the first stage, compression waves produced by the accelerating flame steepen into the shock far ahead from the flame front, at  $(X_{sh} - X_f) \sim (5-10)D$ , during the second stage the compression wave produced by the flame steepens into the shock close to the surface of the flame, which acts as a piston [11].

### 3 Formation of the Large Amplitude Pressure Pulse and DDT

Accelerating flame acts as a piston, producing compression waves ahead, so that the flow is not isobaric. When the compression waves steepen to the shock close to the flame (the stage of decreasing acceleration for wide channels), the unreacted mixture of increased density starts entering the flame. It is heated inside of the flame front and produces a pressure pulse on the scale of the order of the flame width. The increased pressure enhances reaction rate and the heat release in the reaction zone creating a positive feedback coupling between the pressure pulse and the reaction rate. As a result the peak of the pressure pulse grows exponentially. In a thin channel the flame velocity increases exponentially all the time, and the compression wave steepens to form a shock at the distance about several widths of the channel. But because of the small width, the distance between the flame and the shock is comparable to the flame thickness. Therefore, in a thin channel the pressure pulse is also formed at the flame front and exponentially increases with time from the beginning. Sequences of the temperature (dashed lines) and pressure (solid lines) profiles corresponding to leading point in the flame front presented in figure 3 show evolution of the pressure peak before the actual transition to detonation in channels  $D = 5\text{mm}$  (left) and  $D = 1\text{mm}$  (right).

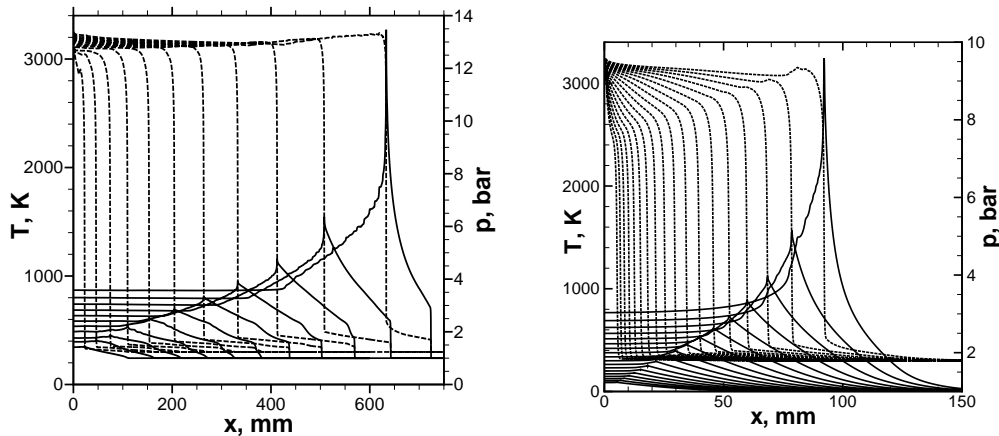


Figure 3. Temperature (dashed lines) and pressure (solid lines) profiles corresponding to leading point in the flame front represent the flame structure and the pressure peak formation. Left:  $D = 5\text{mm}$ ,  $t_0 = 0.2\text{ms}$ ,  $t_f = 1.2\text{ms}$ ,  $\Delta t = 0.1\text{ms}$ . Right:  $D = 1\text{mm}$ ,  $t_0 = 0.1\text{ms}$ ,  $t_f = 0.3125\text{ms}$ ,  $\Delta t = 0.0125\text{ms}$ .

The last stage of the actual transition to detonation is shown in figure 4, which presents variations of the pressure, temperature and concentration  $Y_H$  of H-radicals profiles at sequential times, from  $t=1.2101875\text{ms}$  till  $1.2113125\text{ms}$  with the time interval  $0.25\mu\text{s}$  for channel  $D=5\text{mm}$ . From  $1.21\text{ms}$  to  $1.211\text{ms}$  the pressure peak steepens into a strong shock which is coupled with the reaction zone forming overdriven detonation. The transition to detonation is clearly seen from the increased temperature gradient and temperature of the products. One can see that the distribution of H-radicals in the reactions is different during the deflagration and after the transition to detonation. In deflagration the H-radicals appears within the deflagration wave, while structure of the detonation wave consists of the well pronounced shock wave with the jump in temperature and pressure following by the reaction.

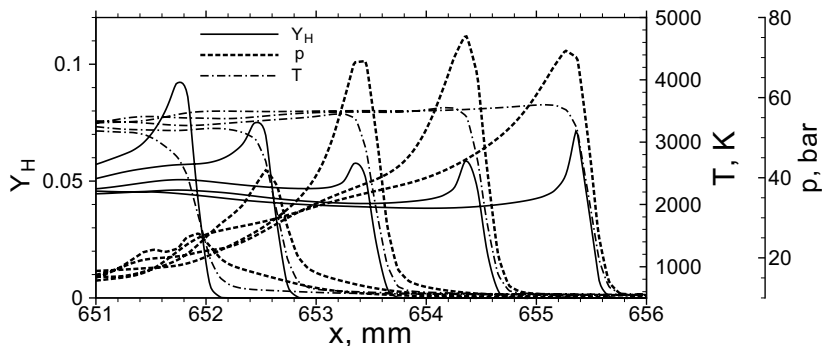


Figure 4. Pressure, temperature and H-radical concentration distributions in the leading point in the flame front during the actual transition to detonation in the channel  $D=5\text{mm}$  from  $1.211\text{ms}$  till  $1.21187\text{ms}$ ,  $\Delta t = 0.125\mu\text{s}$ .

In a thin capillary channels the mechanism of DDT is similar to that in a wide channel except of some details of the detonation wave which is formed after the transition. In contrast to a wide channel in a narrow channel there is no shocks, which run ahead and compress the gas far ahead of the flame. Therefore in a narrow channel the Chapman Jouguet detonation is formed almost bypassing the stage of an overdriven detonation. The characteristic detonation cell size in hydrogen/oxygen at atmospheric pressure is  $2.5\text{mm}$ , which is larger than the channel width. Therefore in a thin channel with the width of the channel less than the detonation cell size a steady detonation wave can not be properly formed. This is presumably manifested by the pressure and density oscillations seen as the density spikes.

## 5 Conclusions

The major conclusion is that the flame acceleration in tubes with no-slip walls is important factor in creating the right conditions for DDT to occur. Effects of the channel width on the dynamics of reaction wave propagating in the channels of different widths from  $0.5\text{mm}$  to  $10\text{mm}$  have been systematically investigated. The critical width of the channel was obtained for hydrogen/oxygen mixture at the atmospheric initial pressure and extrapolated for ethylene-oxygen. Insight into how DDT occurs and what is the mechanism of DDT was obtained by analyzing a long series of high resolution numerical simulations with a detailed chemical reaction model. It is shown that the shock formed close to the flame front is the primary factor for generating exponentially growing large amplitude pressure peak which start-up mechanism of DDT. This exponentially growing pressure pulse then triggers the transition to detonation. The auto-ignition delay times for temperatures in the mixture ahead of the flame in a 'hot' spot and the like are far too long to contribute to any purely thermal ignition phenomenon. This means the transition to detonation can't be evolved due to the formation of a 'hot spot' and the like with a gradient in auto-ignition delay that satisfied the Zel'dovich criterion at least for highly reactive mixtures.

---

## References

- [1] Schelkin, K. I. (1940) Influence of the wall roughness on initiation and propagation of detonation in gases, *Zh. Eksp. Teor. Fiz.* (in Russian) Vol. 10: 823 .
- [2] Jones, H. (1958) Accelerated flames and detonation in gases, *Proc. Roy. Soc. A*242: 333.
- [3] Shchelkin, K. I. and Troshin, Ya. K. (1965) *Gasdynamics of Combustion*, Mono Book Corp. Baltimore.
- [4] Zel'dovich, Ya. B. and Kompaneets, A.S. (1960) *Theory of Detonation*, Academic press, New York.
- [5] Oppenheim, A.K. and Soloukhin, R. I. (1973) Experiments in gasdynamics of explosion, *Ann. Rev. Fluid Mech.* Vol. 5: 31.
- [6] Shepherd, J. E., and Lee, J. H. S. (1992) On the transition from deflagration-to-detonation, in *Major Research Topics in Combustion* (M. Y. Hussaini, A. Kumar, and R. G. Voigt, eds), Springer-Verlag, New York, pp. 439-487.
- [7] Smirnov, N.N. and Nikitin, V.F. (2004) Effect of channel geometry and mixture temperature on deflagration-to-detonation transition in gases, *Combustion, Explosion, and Shock waves*, Vol. 40: 186.
- [8] Dobrego, K.V., Kozlov, I.M., Vasiliev, V.V. (2006) Flame dynamics in thin semi-closed tubes at different heat loss conditions, *Int. J. Heat and mass transfer*, Vol.49: 198.
- [9] Ming-hsun Wu, Burke, M.P., Son, S.J., Yatter, R.A. (2007) Flame acceleration and the transition to detonation of stoichiometric ethylene/oxygen in microscale tubes, *Proceedings of the Combustion Institute*, 31: 2429.
- [10] Kuznetsov, M. (2010) Flame acceleration and the transition to detonation of stoichiometric hydrogen/oxygen in rectangular tubes 1-5mm, private communication.
- [11] Liberman, M.A. et al. (2010) Deflagration-to-detonation transition in highly reactive combustible mixtures, *Acta Astronautica*, Vol. 67: 688-701.
- [12] Liberman, M.A. et al. (2010) On the Mechanism of the Deflagration-to-Detonation Transition in a Hydrogen–Oxygen Mixture, *Zh. Exp. Theor. Fiz. (JETP)* 138: 772-788.
- [13] Ivanov, M.F., Kiverin A.D., Liberman, M.A. (2010) Flame Acceleration and Deflagration-to-Detonation Transition in Stoichiometric Hydrogen/Oxygen in Tubes of Different Diameters, *Combust. Flame*, submitted.
- [14] Clanet, C., Searby, G. (1996) On the “Tulip Flame” Phenomenon, *Combust. Flame* 105: 225.
- [15] Landau, L. D. and Lifshitz, E. M. (1989) *Fluid Mechanics*, Pergamon Press, Oxford.
- [16] Kuznetsov, M., Liberman, M., Matsukov I. (2010) Experimental Study of the Preheat Zone Formation and Deflagration to Detonation Transition, *Combust. Sci. Tech.* 182: 1628.